International Journal of Pharmaceutics 388 (2010) 129–135

Contents lists available at ScienceDirect

International Journal of Pharmaceutics

journal homepage: www.elsevier.com/locate/ijpharm

Erythritol: Crystal growth from the melt

A.J. Lopes Jesus [a,b,*], Sandra C.C. Nunes [b], M. Ramos Silva [c], A. Matos Beja [c], J.S. Redinha [b]

[a] Faculty of Pharmacy, University of Coimbra, 3004-295 Coimbra, Portugal
[b] Department of Chemistry, University of Coimbra, 3004-535 Coimbra, Portugal
[c] Department of Physics, University of Coimbra, 3004-516 Coimbra, Portugal

ARTICLE INFO

Article history:
Received 15 September 2009
Received in revised form
18 December 2009
Accepted 22 December 2009
Available online 5 January 2010

Keywords:
Erythritol
Crystallization from melt
Crystalline and amorphous phases
Metastable form
Thermal methods
Powder X-ray diffraction and infrared spectroscopy

ABSTRACT

The structural changes occurring on erythritol as it is cooled from the melt to low temperature, and then heated up to the melting point have been investigated by differential scanning calorimetry (DSC), polarized light thermal microscopy (PLTM), X-ray powder diffraction (PXRD) and Fourier transform infrared spectroscopy (FTIR).

By DSC, it was possible to set up the conditions to obtain an amorphous solid, a crystalline solid, or a mixture of both materials in different proportions. Two crystalline forms have been identified: a stable and a metastable one with melting points of 117 and 104 °C, respectively. The fusion curve decomposition of the stable form revealed the existence of three conformational structures.

The main paths of the crystallization from the melt were followed by PLTM. The texture and colour changes allowed the characterization of the different phases and transitions in which they are involved on cooling as well as on heating processes. The type of crystallization front and its velocity were also followed by microscopic observation. These observations, together with the data provided by PXRD, allowed elucidating the transition of the metastable form into the stable one.

The structural changes occurring upon the cooling and subsequent heating processes, namely those arising from intermolecular hydrogen bonds, were also accompanied by infrared spectroscopy. Particular attention was given to the spectral changes occurring in the OH stretching region.

1. Introduction

Erythritol, a meso-compound of 1,2,3,4-butanetetrol, is a natural occurring sugar alcohol presented in various fruits and fermented foods, as well as in body fluids of humans and animals. Industrially, it is prepared by glucose fermentation. Due to its good thermal stability, very low hygroscopicity (Cohen et al., 1993), sweetness taste, low toxicity (Munro et al., 1998), and high compatibility with drugs (Zhou et al., 2000), it became an ideal excipient to be used in pharmaceutical formulations (Ohmori et al., 2004; Endo et al., 2005; Gonnissen et al., 2007). For example, recent studies demonstrate that this compound is a more appropriate material for thin-layer sugarless coating, when compared with other polyols (Ohmori et al., 2004). It has also advantages over other excipients in the adhesion of drugs to be used as carrier excipient (Traini et al., 2006). Moreover, its low caloric content (0.2 kcal/g, 70% of that of sucrose) and anti-cariogenic properties make it largely used as sugar substitute in the widespread market of light and reduced calories products (Haji, 2007, 2008).

Since melt extrusion is a process that has been increasingly used in the preparation of pharmaceutical dosage forms (Ndindayino et al., 2002; Crowley et al., 2007; Repka et al., 2007, 2008), the prior knowledge of the thermal behaviour of this compound, namely when it is cooled from the melt, assumes a great importance. Some studies on phase and state transitions in polyols, including erythritol, have been performed (Talja and Roos, 2001). Nevertheless, in view of the role of this compound in the pharmaceutical industry, a deep insight into its structure upon cooling and subsequent heating processes is required.

In the present paper, the structural modifications occurring on cooling erythritol from the melt to low temperature and on subsequent heating till fusion were studied by differential scanning calorimetry (DSC), polarized light thermal microscopy (PLTM), X-ray powder diffraction (PXRD) and Fourier transform infrared spectroscopy (FTIR). The combination of these four well established methods for solid state research proved to be very useful as they provided complementary informations.

2. Experimental

Erythritol used in the present work was of the best grade commercially available product (Fluka, >99%). The purity of the compound was checked by gas/liquid chromatography (Jesus et al.,

* Corresponding author at: Faculty of Pharmacy, University of Coimbra, 3004-295 Coimbra, Portugal. Tel.: +351 239488400; fax: +351 239827126.
E-mail address: ajorge@qui.uc.pt (A.J.L. Jesus).

0378-5173/$ – see front matter © 2009 Elsevier B.V. All rights reserved.
doi:10.1016/j.ijpharm.2009.12.043

2005). A purity degree of 99.9% has been assigned to the compound under study. Before using, the compound was dried under vacuum at 80 °C. To be used as a reference, a certain amount of erythritol was further recrystallized from aqueous solution and dried over several days.

DSC determinations were conducted with a power compensation Perkin-Elmer Pyris 1 instrument equipped with a liquid nitrogen cryofill cooling unit. Helium (purity >99.999%) was used as purge gas at a 20 mL/min flow rate. The samples (2–4 mg) were hermetically sealed in 40 μL aluminium pans suitable for volatile substances. An empty pan prepared on the same way was used as reference. Temperature calibration was performed with cyclopentane (Merck, $x > 99.7\%$, $T_{fus} = -93.43$ °C), cyclohexane (Merck, $x > 99.7\%$, $T_{fus} = 6.66$ °C), biphenyl (SRM, LGC 2610, $T_{fus} = 80.20$ °C), benzoic acid (SRM, LGC 2606, $T_{fus} = 122.85$ °C) and indium (Perkin-Elmer, $x > 99.7\%$, $T_{fus} = 156.60$ °C). Enthalpy calibration was performed with indium ($\Delta H_{fus} = 3286\ J\ mol^{-1}$). Fresh samples were firstly heated from 25 to 140 °C at a scanning rate of 10 °C min^{-1}. The liquid was then cooled down to −170 °C and the frozen material was heated again to 140 °C. All heating/cooling cycles were performed at different scanning rates (from 0.5 to 50 °C min^{-1}). The Perkin-Elmer Pyris software (version 3.5) was used to analyse and plot the thermal data.

Powder X-ray diffraction experiments were conducted using an Enraf-Nonius powder diffratometer equipped with a CPS120 detector and a quartz monochromator. A Cu Kα_1 radiation ($\lambda = 1.5406$ Å) was selected for data collection. Temperature variation of the sample was obtained with a 700 series Cryostream—Oxford Cryosystems, tested previously by performing data collections with hexamethylbenzene and cyclohexane. The data were calibrated to convert the measured channels to 2θ by means of cubic spline fittings to the peaks of silicon (with the direct beam position added), used as an external calibrant. Erythritol crystals were powdered thoroughly and a glass capillary of 0.3 mm diameter was filled with powder. The capillary was placed in a goniometer head and both heated in an oven at 150 °C. They were then quickly transferred to the diffractometer with the nitrogen open flow cryostat running and set to −123 °C. Diffractograms of the frozen solid were recorded at different temperatures from this temperature on.

The instrumentation used in the PLTM determinations consisted of a DSC600 hot/cold stage manufactured by Linkam Scientific Instruments Ltd., associated to a DMRB Leika microscope. Images of the sample, observed under polarized light, were recorded using a Sony CCD-IRIS/RGB video camera. A Linkam system software with a Real-Time Video Measurement System was used for image analysis. The images were obtained by combined use polarized light and wave compensators, using a 200× magnification. Temperature accuracy readings were checked out with the melting points of benzophenone (Metler Toledo calibration substance ME 18,870, $T_{fus} = 48.1 \pm 0.2$ °C) and benzoic acid (SRM, LGC 2606, $T_{fus} = 122.85$ °C).

Small pieces of the sample were spread over the bottom of a covered glass cell. The cover was placed directly over the sample in a thin flat preparation. Upon fusion, the solid pieces originate liquid drops which have been observed during cooling and heating runs. A few drops were focused in the microscope field, allowing simultaneous observation of events in various separated drops. The experiments were performed under nitrogen atmosphere.

The infrared spectra of the solid erythritol dispersed in a KBr matrix were recorded between 4000 and 400 cm^{-1} in a temperature range from −170 to 140 °C. A Graseby Specac cell within ±1 °C temperature control was used. Liquid nitrogen was employed as cooling agent. The spectra were recorded on a Thermo Nicolet IR 300 spectrometer, with 1 cm^{-1} spectral resolution. The spectra were acquired with 128 scans and data acquisition was performed with the EZ OMNIC 6.1a (Thermo Nicolet Corporation, USA) software.

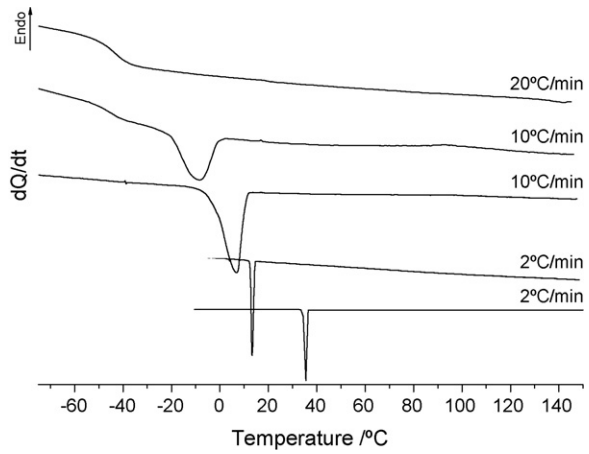

Fig. 1. Typical cooling DSC curves for erythritol growing from melt at different scanning rates.

3. Results and discussion

3.1. Differential scanning calorimetry (DSC)

Upon cooling the melt, two types of transitions can be observed, depending, in a certain extension, on the rate at which the process is run. As can be seen in Fig. 1, at 2 °C min^{-1}, the unique perceptible phase transformation is that corresponding to the liquid crystallization. The same thermal event is observed using other slow scanning rates (1 and 5 °C min^{-1}, not shown in Fig. 1). This process is characterized by one or two exothermic DSC signals occurring between 16 and 14 °C, or, in a few cases, at temperatures around 40 °C. The corresponding enthalpy values lie between −20 and −21 kJ mol^{-1}. Conversely, cooling at a high rate (20 °C min^{-1}), only a glass transition is observed. This transition takes place at temperatures between −42 and −46 °C, with a heat capacity variation of about 0.1 J K^{-1} mol^{-1}. At intermediate cooling rates (10 °C min^{-1}) both transitions referred above are generally observed. The crystallization temperature varies from 45 to 3 °C and the values obtained for the enthalpy lie between 0.2 and 22 kJ mol^{-1}. This wide range of values reflects the different structural ordering exhibited by the solid formed under these conditions.

Important structural informations can also be drawn upon heating the solid grown from the melt. In Fig. 2 are shown some DSC curves corresponding to the subsequent heating runs at 10 °C min^{-1} for solids obtained from the liquid at different cooling rates. A similar thermal behaviour has been observed using other heating rates (see supplementary material). While the specimens cooled at low rates (≤5 °C min^{-1}) do not show thermal manifestations on heating but fusion, those crystallized at moderate rates exhibit a glass transition at a temperature around −44 °C and one or two exothermic peaks of crystallization between −20 and 20 °C. The enthalpy of crystallization on heating depends on the value obtained for this property on cooling. The sum of the two values is approximately −22 kJ mol^{-1}. In absolute terms, this figure is close to that obtained for the enthalpy of fusion accounting for the thermal correction due to the temperature difference between the two-phase transitions (Jesus et al., 2005).

On heating, most of the frozen solids exhibit a peak of fusion with $T_e = 117$ °C (extrapolated onset temperature) and $\Delta H_{fus} = 39\ kJ\ mol^{-1}$. These values are very close to those reported in literature (Barone et al., 1990) and to those obtained in the present work for erythritol recrystallized from water ($T_{fus} = 117.8$ °C

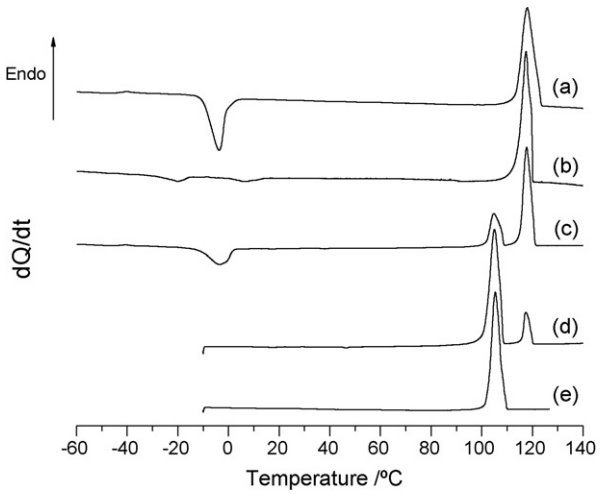

Fig. 2. DSC heating curves of erythritol (frozen solid) at 10 °C min^{-1} obtained by cooling from the melt at 20 °C min^{-1} (a), 10 °C min^{-1} (b) and (c), 2 °C min^{-1} (d) and 0.5 °C min^{-1} (e).

and ΔH_{fus} = 39.4 kJ mol^{-1}). Occasionally, another peak of fusion is observed with T_e = 104 °C (see curves c, d and e in Fig. 2). This can be the unique observable fusion peak ($\Delta H_{fus} \approx 34$ kJ mol^{-1}), or can appear together with the higher temperature one. In the latter case, the ratio of their areas varies from 0 to 1. These results indicate that the frozen erythritol originates two forms: one melting at 117 °C and the other 13 °C below. According to the heat of fusion rule (Burger and Ramberger, 1979) the two forms are likely to be monotropically related with that of higher melting point being the stable one over all temperature range before fusion.

A point to be further considered into the discussion of the calorimetric results is that concerned with the profile of the fusion curve occurring at higher temperatures. In fact, the fusion peaks are too wide (base-width of the peak falling between 15 and 20 °C) and present a round maximum. These features are likely attributed to the existence of more than one pure conformational form. To clarify this point, the DSC peaks were analysed by peak fitting using a parametric modified Gaussian equation worked out by Leitão et al. (2002). The best fit was achieved by decomposition of the fusion peak into two or three individual Gaussian curves as represented in Fig. 3.

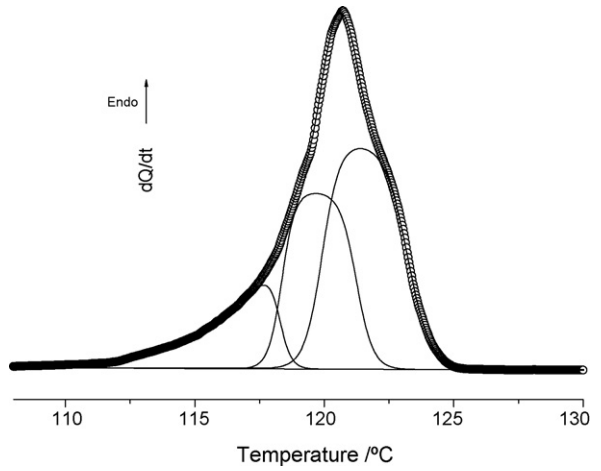

Fig. 3. Result of the peak fit analysis of the fusion curve of frozen erythritol occurring at 117 °C. The DSC heating curve was traced using a scanning rate of 10 °C min^{-1}. Values of T_p of the deconvoluted peaks: 118.1, 119.6 and 121.3 °C. Fitting quality parameters: Chi-square = 0.045507 and r = 0.99995.

The values of the peak maximum temperature (T_p) of the overlapped curves were grouped into clusters using the K-means method. The extrapolated onset temperature is commonly adopted for the melting point of a compound as it is less affected by the scanning rate than T_p. Nevertheless, when the curve results from the overlap of various components the last parameter may be more accurate and more easily determinated than the former.

Different number of clusters (K) was considered in the statistical distribution of T_p. The criterion used to establish the number of clusters was such that no significant decrease in the variance within each cluster was observed by increasing K. In our case K = 3 fulfilled this requirement. The mean values and uncertainties of T_p for the three clusters and the number of cases (n) falling in each of them are the following: T_p = 118.5 ± 0.5 °C (n = 8), T_p = 119.9 ± 0.4 °C (n = 19), T_p = 122.1 ± 0.7 °C (n = 18).

From the analysis of the fusion curves one can say that crystalline erythritol presents three conformational structures. Most specimens are constituted by structures with T_p = 119.9 and 122.1 °C, both with identical probabilities. The conformational structure with T_p = 118.5 °C has only 18% probability of occurrence. These results are consistent with the neutron diffraction data that show the existence of conformational disorder around the middle C–O bonds in the crystalline structure (Ceccarelli et al., 1980). Since a unique unit cell is found to exist, the solid erythritol can be considered as an isomorphic conformational structure.

3.2. Powder X-ray diffraction (PXRD)

As expected from the DSC experiments, a rapid cooling of the liquid erythritol originates an amorphous phase. In fact, the X-ray diffraction pattern of the solid obtained under these conditions exhibits a very diffuse peak with a maximum at 2θ = 20°, as shown in the diffractogram A of Fig. 4. Sometimes, a well defined peak at 2θ = 21° and other small ones at 2θ = 38 and 41° are also observed (diffractogram A′). This type of pattern with very few strong reflections at low angles is characteristic of an orientational disordered material, with only the centres of mass of the molecules fixed in

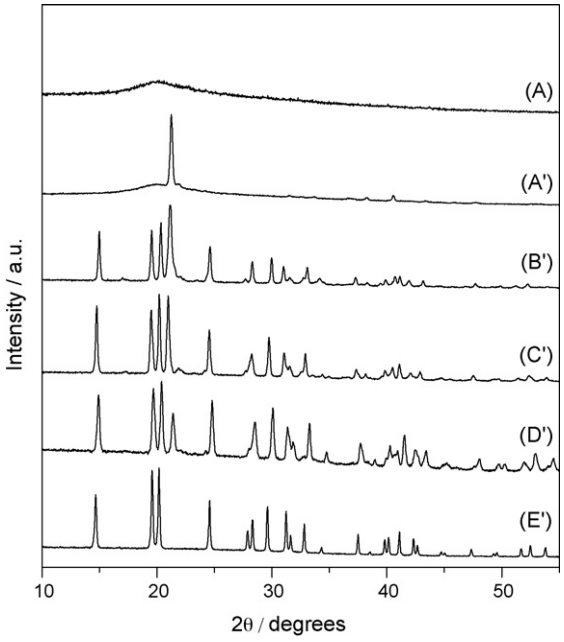

Fig. 4. X-ray powder diffraction patterns of erythritol obtained under different conditions. A and A′: at −70 °C by quenching the molten erythritol; B′ and C′: upon heating the frozen solid (diffractrogram A′) at −8 and 20 °C, respectively; D′ and E′: after leaving the solid at 20 °C for 3 and 12 h, respectively.

a lattice. In any case, as the temperature reaches approximately −10 °C, the broad peak is replaced by numerous narrow peaks with the most intense ones located at $2\theta = 15°$, 19.5°, 20.3° and 24.6° (diffractogram B′). This change indicates that the amorphous solid is transformed into a new crystalline phase. At this temperature, the X-ray diffraction pattern of the solid erythritol is that characteristic of this crystalline form, sometimes with an extra peak ($2\theta = 21°$) corresponding to that arisen on quenching. That is, the amorphous part of the quenched material becomes crystalline and that already exhibiting some crystallinity remains unchanged. As the temperature increases to 20 °C, no significant change in the diffraction pattern is observed but only a better definition of the peaks (diffractogram C′).

The solid was then left at this temperature for several hours and different diffractrograms were recorded along the time. After 3 h, a decrease of the intensity of peak at $2\theta = 21°$ is clearly shown (diffractogram D′), disappearing after 12 h (diffractogram E′). These observations confirm that the primitive crystalline phase formed by rapid cooling of the melt, and identified by DSC as melting at 104 °C, is metastable. It can be converted into the stable one with time.

Diffractogram E′ corresponds exactly to the calculated powder diffractogram from the single crystal data (Ceccarelli et al., 1980) with cell parameters $a = b = 12.713$ Å, $c = 6.747$ Å, $V = 1090.5$ Å^3 and space group $I4_1/a$. Diffractogram A′ corresponds to a unit cell with smaller volume, since the first reflection is only seen at 21°. Peak indexing is not possible due to the scarcity of reflection lines.

3.3. Polarized light thermomicroscopy (PLTM)

The solid phase originated from the melt, observed under polarized light, shows to be partially or totally crystalline, when moderate (10 °C min^{-1}) or low cooling rates (<5 °C min^{-1}) are used. Generally, an anisotropic solid phase is obtained from the liquid at a temperature between 10 and −10 °C. At a cooling rate of 1 or 2 °C min^{-1} the crystallization of the supercooled liquid is apparently complete, whereas at 20 or 50 °C min^{-1}, an amorphous solid is obtained. At 10 °C min^{-1}, two phenomena can occur: sometimes, the solid is like that formed at low rates; in some others, crystalline and glassy phases can be observed together. Once in a while, the solidification takes place at a lower supercooling (50–30 °C). Each of the events just described will be discussed in detail below.

The main paths of the crystallization process at higher supercooling can be followed by the micrographs shown in Fig. 5. In the case illustrated in Fig. 5A, using a cooling rate of 2 °C min^{-1}, the solidification of the melt is initiated at 11 °C inside the liquid drop and the nucleus of the new phase rapidly grows towards the surface. The crystallization front gives rise to a mushy region, which in turns, is transformed, into a grained texture. The solid exhibits fractures oriented perpendicularly to the growth direction.

Image analysis allows the characterization of the solid growth front and the determination of the velocity of crystallization (VC). Both are important features in the crystallization process. The variation of the position of the solid/liquid interface as function of time (curve A) and the corresponding values of the velocity of crystallization (curve A′) are represented in Fig. 6.

The outbalance between the heat released in the nucleation of the new phase and its sequent removal from the medium disturbs the steady-state conditions, giving rise to supercooling fluctuations large enough to produce interface instability (Jackson, 1975; Buyevich et al., 2000). A self-oscillating crystallization front is then observed.

When the crystallization front reaches an outer liquid region of about 50 μm the crystallization shows a rather different pattern. A grained texture results straight from the liquid without any intermediate interfacial texture being formed.

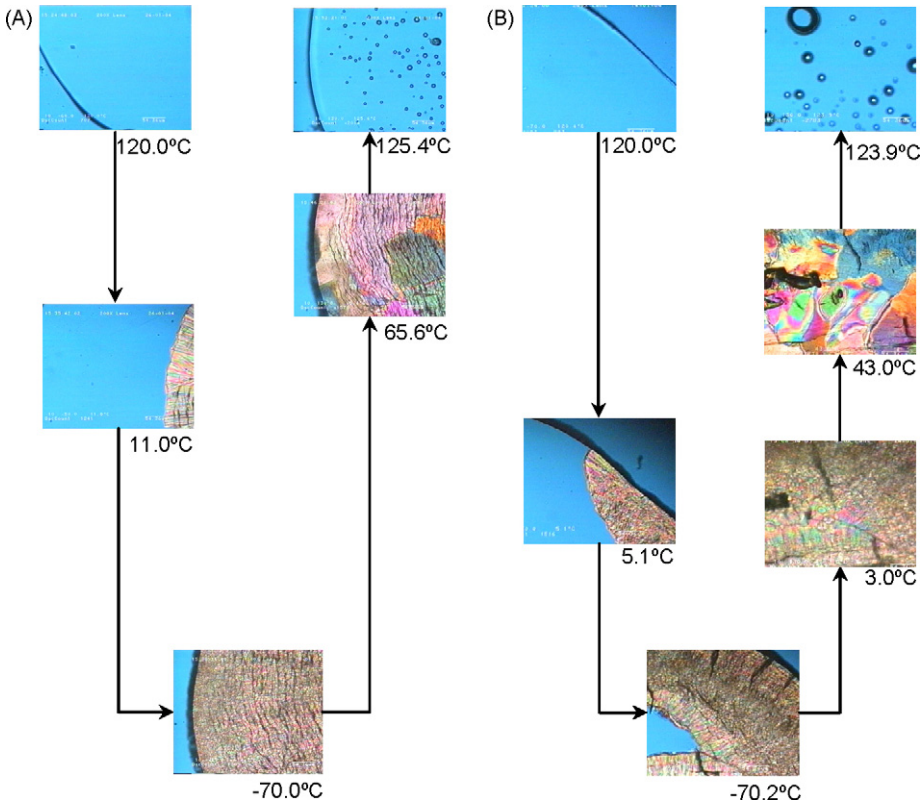

Fig. 5. Hot-stage polarized micrographs at different temperatures representing the main important transformations occurring upon cooling the molten erythritol at 2 °C min^{-1} (A) and 10 °C min^{-1} (B), down to −70 °C, followed by heating up to the melting point at 10 °C min^{-1}.

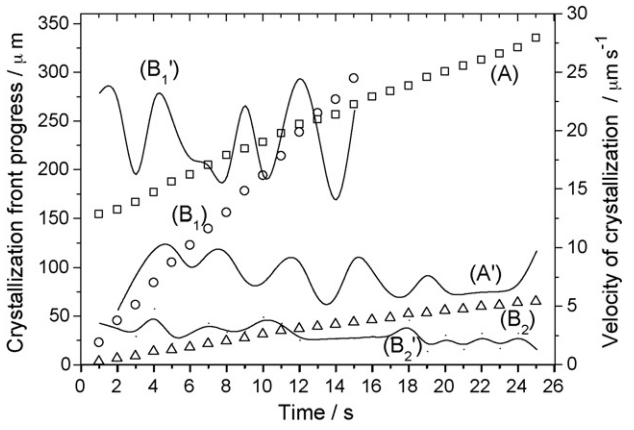

Fig. 6. Crystallization front progress (A, B_1 and B_2) and velocity of crystallization (A′, B'_1 and B'_2) as function of time in the solidification of erythritol on cooling from the melt. Values of A and A′ were taken from the mechanism (A) of Fig. 5; B_1/B'_1 from mechanism (B) with the nucleation occurring at the surface; B_2/B'_2 from the same mechanism but with the nucleation inside the liquid drop.

Two types of behaviour are exhibited as the frozen solid is heated at 10 °C min^{-1}. In the most frequent one, the grains become roundish and the texture more compact. At about 65 °C, a solid/solid transformation takes place (see micrograph at 65.6 °C). The nucleation of a new phase occurs in several points of the solid and each nucleus grows, giving a phase boundary texture. The value of VC for this transformation is about 30 μm s^{-1}. Since no heat is involved, as revealed by DSC, it is fundamentally an entropically driven process. This transformation takes place through a diffusional process, what means that it occurs by defect movement in the lattice. In this mechanism, a vacancy or interstitial site is exchanged for another, undergoing a jump in the lattice network (Ropp, 2003). The self-diffusion coefficient is much higher than a normal diffusion in a solid as it is indicated by the relative high rate of this transition. The resulting structure melts at a temperature of about 120 °C, giving rise to a liquid phase with numerous air bubbles resulting from the void spaces existent in the solid. This is a common feature for erythritol prepared on cooling the liquid. Occasionally, the solid/solid transformation on the heating run is bypassed and the fusion occurs at about 104 °C.

An alternative type of crystallization with the same supercooling as that described above is illustrated in Fig. 5(B) using a cooling rate of 10 °C min^{-1}. The embryo of the solid phase occurs on the surface of a liquid drop. The nucleus growth along the surface is much faster than that towards the centre. Indeed, while VC is 20 ± 5 μm s^{-1} in the crystallization of a superficial liquid layer of 50 μm thick (curve B'_1 in Fig. 6), VC towards the centre of the liquid drop is about 2.5 μm s^{-1} (curve B'_2). The crystallization front at the surface is different from that towards the interior of the liquid drop. Indeed, while in the first the liquid gives directly a coarse grained solid texture, in the second, a mushy solid is initially formed, which is quickly transformed into a cracking fine grain texture.

As a consequence of the faster crystallization of the outer liquid at the end of the cooling process, the solid has a crystalline shell involving a glassy core (see micrograph at −70.2 °C). Amorphous and crystalline phases are distinct domains of the solid.

On heating the solid at 10 °C min^{-1}, the disordered material begins to crystallize at −8 °C through two simultaneous processes: crystal growth on the solid/liquid interface and spherulites formation (Emons et al., 1982) in the fluid resulting from the glass devitrification. The crystallization on heating ends at about 2.5 °C. A solid/solid transformation, occurring between 15 and 43 °C, is then observed. Although this transition is much slower than that described above, the texture modifications are similar. The fine specks are sintered into particles which grow until impingement. These particles show different colours under polarized light. The diversity of colours indicates that the crystallites in one particle have different orientations from that of its neighbours (Ropp, 2003) (see micrograph at 43 °C). The final solid melts at about 120 °C.

By last, the crystallization on cooling can also occur at a lower supercooling, generally at a temperature between 50 and 30 °C (Fig. 7). The solid formed has a dendritic texture (Ananth and Gill, 1991; Pines et al., 1999) and the crystallization is fast (VC > 100 μ ms^{-1}). Once again, the frozen solid can have two distinct behaviours upon heating. In one case, a further recrystallization takes place at about 75 °C and the final crystalline form melts at about 120 °C. This solid/solid transformation is characterized by a fast diffusional process originating also a boundary texture. Alternatively, the solid obtained by cooling the melt does not recrystallize on heating and the fusion occurs approximately at 104 °C.

PLTM gave a valuable contribution to the study of the temperature effect on the structure of erythritol. Besides the support given to the DSC data, it allowed a deeper interpretation on the phases and the transformations in which they are involved, some of them not detected by DSC. A metastable form exhibiting various solid textures is formed upon cooling. In the subsequent heating, this form is converted into the stable one providing a solid/solid transformation occurs. This transformation could only be followed by PLTM.

3.4. Fourier transform infrared spectroscopy (FTIR)

The protocol established in this research for the study of erythritol was also followed by infrared spectroscopy. Since H-bonds are the dominant intermolecular interactions in the solid, special attention was given to the OH vibrations, in particular to those occurring in the stretching region, since they are the most sensitive ones to structure variations.

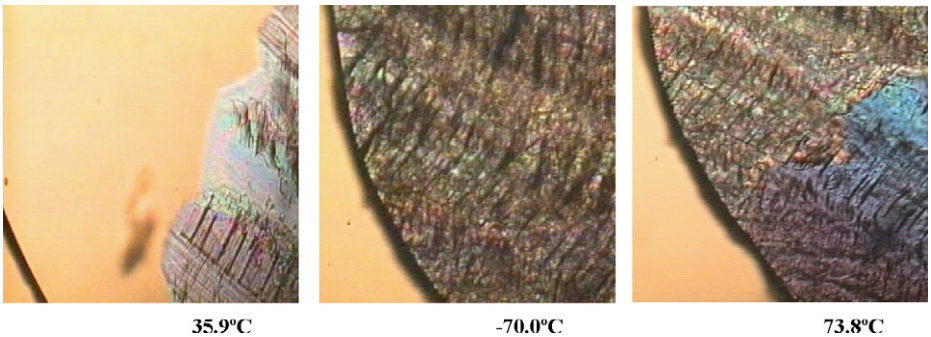

Fig. 7. Hot-stage polarized micrographs illustrating the most important transformations on cooling from the melt (two left micrographs) and subsequent heating (right micrograph) when crystallization occurs at lower supercooling. Cooling and heating rates were performed at a scanning rate of 10 °C min^{-1}.

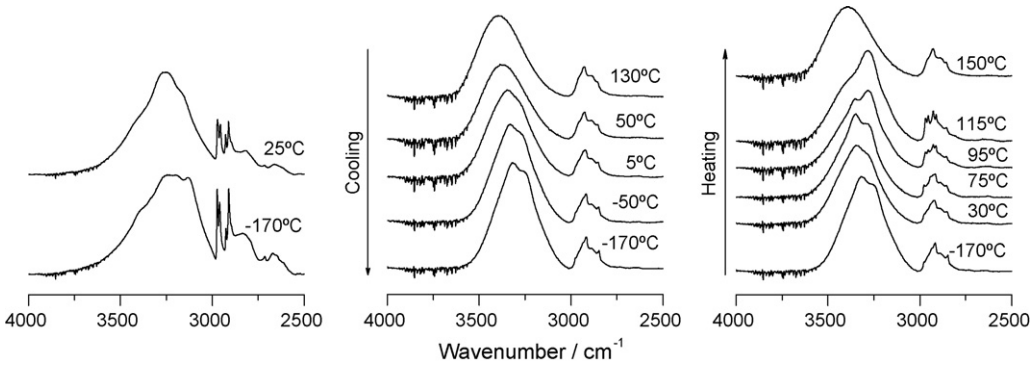

Fig. 8. Infrared spectra of erythritol in the OH and CH stretching regions at different temperatures and under different conditions. Left spectra: original erythritol; middle spectra: cooling from the melt down to −170 °C; right spectra: heating the frozen solid up to fusion.

Fig. 8 depicts spectra of erythritol in the 4000–2500 cm^{-1} region at different temperatures. The main spectral changes when the melt is cooled down to −170 °C can be followed through the spectra shown in the middle panel, while in the right panel are represented the spectra obtained during the subsequent heating. To be used as reference, two spectra of erythritol recrystallized from aqueous solution traced at 25 and −170 °C are also shown (left panel).

At 130 °C, the compound is in the liquid state and the spectrum exhibits a broad band with $\nu_{max} \approx 3400\,cm^{-1}$. This is characteristic of an associated liquid since the stretching vibration of a free OH group in hydroxyl compounds is around 3630 cm^{-1} (Fishman and Chen, 1969; Jesus et al., 2003, 2006). Thus, all OH groups are involved in intermolecular H-bonds and no distinction between them can be made. Upon cooling, as the temperature reaches 5 °C, the absorption band becomes asymmetric and two strongly overlapped bands appear, becoming better defined as the temperature decreases. At −170 °C, the spectrum of the solid erythritol presents two bands with ν_{max} at 3346 and 3243 cm^{-1}. Apparently, the structure of the frozen solid is characterized by two distinct intermolecular H-bonds systems. At the same temperature, the spectrum of solid erythritol recrystallized from aqueous solution exhibits a rather complex pattern. Three fundamental OH stretching bands have been identified and assigned to the same number of intermolecular H-bonds (Jesus and Redinha, 2009). The two structures are significantly different in respect with the number of intermolecular H-bonds. Also, the CH stretching bands of the spectra of the frozen solid are less structured.

Let us now consider the spectral modifications of the frozen solid as it is heated up to the melting point. To better visualize these changes, the variation of the peak maximum (ν_{max}), width at half-height ($\Delta\nu_{1/2}$) and intensity (relative area) of the OH stretching bands are represented in Fig. 9. Up to ≈−50 °C, the values of ν_{max} of the bands remain constant and both have similar intensities and $\Delta\nu_{1/2}$ values. Further increasing the temperature, the two peak maxima are slightly shifted to higher frequencies and the lower frequency band becomes less intense than the other. As the temperature reaches 75 °C, the intensity of the higher frequency band starts to decrease and disappears at 95 °C. At this temperature, two new bands appear: one at 3186 cm^{-1} and the other at 3456 cm^{-1}. These spectral variations give evidence for the structure transformations observed by other techniques used in the present investigation.

Just before the melting point (see spectrum at 115 °C in the left panel of Fig. 8), the OH stretching region is composed by three component band whose maxima are located at 3450, 3278 and 3186 cm^{-1}. These maxima are close to those in the spectrum of recrystallized erythritol at 25 °C: 3414, 3256 and 3154 cm^{-1}. Another important feature to be noted is that the bands in the CH stretching region became narrower, resembling those of the reference erythritol (see spectrum at 25 °C in the left panel of Fig. 8).

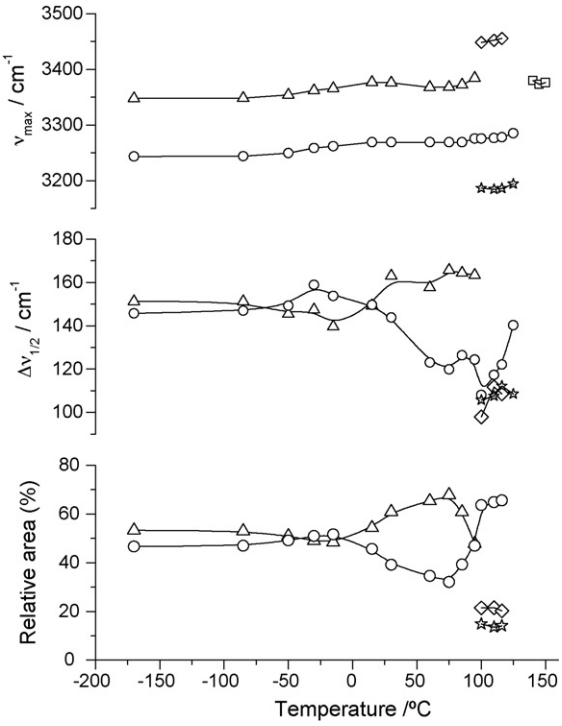

Fig. 9. Variation of the peak maximum (ν), with-at-half-height ($\Delta\nu_{1/2}$) and relative intensities of the OH stretching vibration bands during the heating of the solid erythritol obtained by cooling from the melt (right spectra of Fig. 8).

Based on the FTIR data, one can conclude that the solid erythritol obtained by crystallization from the melt has not a complete intermolecular H-bonds system. Apparently, only two distinct types of H-bonds are distinguishable. On heating, just before fusion, the bands in the OH and CH regions become more structured and their profile becomes similar to that of the recrystallized solid at 25 °C. This means that the solid undergoes a further recrystallization into the original form before fusion takes place, which is in consistent with the general trend observed by PLTM.

4. Concluding remarks

The solid erythritol obtained from the melt has different degrees of crystallization depending, in a certain extension, on the cooling rate. Rapid cooling gives rise to an amorphous form, whereas slow cooling originates a crystalline form. As shown by FTIR, this form

has not a perfect crystalline structure. The stable crystalline form is only obtained upon heating the frozen solid or leaving it for several hours at the room temperature.

Two transitions occur as the solid obtained from the melt is heated: Firstly, the liquid resulting from the disordered solid crystallizes; Secondly, a solid/solid transition is observed before melting which occurs at around 117 °C. This transition was followed by PLTM and also detected by PXRD and infrared spectroscopy. Since it is not manifested by DSC, one can conclude that it is an entropic-driven process. When this transformation is bypassed, the metastable crystalline form melts at about 104 °C.

DSC data also shows that the stable form of erythritol is a mixture of three conformational structures. Having in mind the diffraction X-ray data available in literature, we can conclude that these conformers are isomorphs.

The fractures occurring during the crystallization of the solid, the different behaviour of the crystallization at the surface or inside of the liquid drops and the high value of the diffusion coefficient in the solid/solid transformation are indications that erythritol prepared from the melt has structure defects, in particular at the surface layer of the solid particles. A strained structure arises from the liquid as evidenced by the fractures and from the profile of the CH stretching bands in the infrared spectra of the frozen solid.

Appendix A. Supplementary data

Supplementary data associated with this article can be found, in the online version, at doi:10.1016/j.ijpharm.2009.12.043.

References

Ananth, R., Gill, W.N., 1991. Self-consistent theory of dendritic growth with convection. J. Cryst. Growth 108, 173–189.

Barone, G., Dellagatta, G., Ferro, D., Piacente, V., 1990. Enthalpies and entropies of sublimation, vaporization and fusion of 9 polyhydric alcohols. J. Chem. Soc., Faraday Trans. 86, 75–79.

Burger, A., Ramberger, R., 1979. On the polymorphism of pharmaceuticals and other molecular crystals. I. Mikrochim. Acta II, 259–271.

Buyevich, Y.A., Alexandrov, D.V., Mansurov, V.V., 2000. Macrokinetics of Crystallization. Begell House, New York.

Ceccarelli, C., Jeffrey, G.A., McMullan, R.K., 1980. A neutron-diffraction refinement of the crystal-structure of erythritol at 22.6 K. Acta Crystallogr. B 36, 3079–3083.

Cohen, S., Marcus, Y., Migron, Y., Dikstein, S., Shafran, A., 1993. Water sorption, binding and solubility of polyols. J. Chem. Soc., Faraday Trans. 89, 3271–3275.

Crowley, M.M., Zhang, F., Repka, M.A., Thumma, S., Upadhye, S.B., Kumar Battu, S., McGinity, J.W., Martin, C., 2007. Pharmaceutical applications of hot-melt extrusion. Part I. Drug Dev. Ind. Pharm. 33, 909–926.

Emons, H.H., Keune, K., Seyfarth, H.H., 1982. Chemical microscopy; thermomicroscopy of organic compounds. In: Svehla, G. (Ed.), Wilson and Wilson's Comprehensive Analytical Chemistry, vol. XVI. Elsevier Scientific Publishing Co., Amsterdam.

Endo, K., Amikawa, S., Matsumoto, A., Sahashi, N., Onoue, S., 2005. Erythritol-based dry powder of glucagon for pulmonary administration. Int. J. Pharm. 290, 63–71.

Fishman, E., Chen, T.L., 1969. An investigation of hydrogen bonding characteristics of butanediols. Spectrochim. Acta A 25, 1231–1242.

Gonnissen, Y., Remon, J.P., Vervaet, C., 2007. Development of directly compressible powders via co-spray drying. Eur. J. Pharm. Biopharm. 67, 220–226.

Haji, F., 2007. Sweetener blends with erythritol-reducing sugar is adding value. Wellness Foods Europe 2, 16–20.

Haji, F., 2008. Erythritol: sweet, natural, healthy. Wellness Foods Europe 1, 20–23.

Jackson, K.A., 1975. Theory of crystal growth. In: Hannay, N.B. (Ed.), Treatise on Solid State Chemistry, vol. 5. Plenum Press, New York.

Jesus, A.J.L., Redinha, J., 2009. On the structure of erythritol and l-threitol in the solid state: an infrared spectroscopic study. J. Mol. Struct. 938, 156–164.

Jesus, A.J.L., Rosado, M.T.S., Leitão, M.L.P., Redinha, J.S., 2003. Molecular structure of butanediol isomers in gas and liquid states: combination of DFT calculations and infrared spectroscopy studies. J. Phys. Chem. A 107, 3891–3897.

Jesus, A.J.L., Tomé, L.I.N., Redinha, J.S., Eusébio, M.E., 2005. Enthalpy of sublimation in the study of the solid state of organic compounds. Application to erythritol and threitol. J. Phys. Chem. B 109, 18055–18060.

Jesus, A.J.L., Rosado, M.T.S., Reva, I., Fausto, R., Eusébio, M.E., Redinha, J.S., 2006. Conformational study of monomeric 2,3-butanediols by matrix-isolation infrared spectroscopy and DFT calculations. J. Phys. Chem. A 110, 4169–4179.

Leitão, M., Canotilho, J., Cruz, M., Pereira, J., Sousa, A., Redinha, J., 2002. Study of polymorphism from DSC melting curves; polymorphs of terfenadine. J. Therm. Anal. Calorim. 68, 397–412.

Munro, I.C., Bernt, W.O., Borzelleca, J.F., Flamm, G., Lynch, B.S., Kennepohl, E., Bär, E.A., Modderman, J., 1998. Erythritol: an interpretive summary of biochemical, metabolic, toxicological and clinical data. Food Chem. Toxicol. 36, 1139–1174.

Ndindayino, F., Henrist, D., Kiekens, F., Van den Mooter, G., Vervaet, C., Remon, J.P., 2002. Direct compression properties of melt-extruded isomalt. Int. J. Pharm. 235, 149–157.

Ohmori, S., Ohno, Y., Makino, T., Kashihara, T., 2004. Characteristics of erythritol and formulation of a novel coating with erythritol termed thin-layer sugarless coating. Int. J. Pharm. 278, 447–457.

Pines, V., Chait, A., Zlatkowski, M., Christoph, B., 1999. Equiaxed dendritic solidification in supercooled melts. J. Cryst. Growth 197, 355–363.

Repka, M.A., Battu, S.K., Upadhye, S.B., Thumma, S., Crowley, M.M., Zhang, F., Martin, C., McGinity, J.W., 2007. Pharmaceutical applications of hot-melt extrusion. Part II. Drug Dev. Ind. Pharm. 33, 1043–1057.

Repka, M.A., Majumdar, S., Kumar Battu, S., Srirangam, R., Upadhye, S.B., 2008. Applications of hot-melt extrusion for drug delivery. Expert Opin. Drug Deliv. 5, 1357–1376.

Ropp, R.C., 2003. Solid State Chemistry. Elsevier, New York.

Talja, R.A., Roos, Y.H., 2001. Phase and state transition effects on dielectric, mechanical, and thermal properties of polyols. Thermochim. Acta 380, 109–121.

Traini, D., Young, P.M., Jones, M., Edge, S., Price, R., 2006. Comparative study of erythritol and lactose monohydrate as carriers for inhalation: atomic force microscopy and in vitro correlation. Eur. J. Pharm. Sci. 27, 243–251.

Zhou, L.M., Sirithunyalug, J., Yonemochi, E., Oguchi, T., Yamamoto, K., 2000. Complex Formation between erythritol and 4-hexylresorcinol. J. Therm. Anal. Calorim. 59, 951–960.